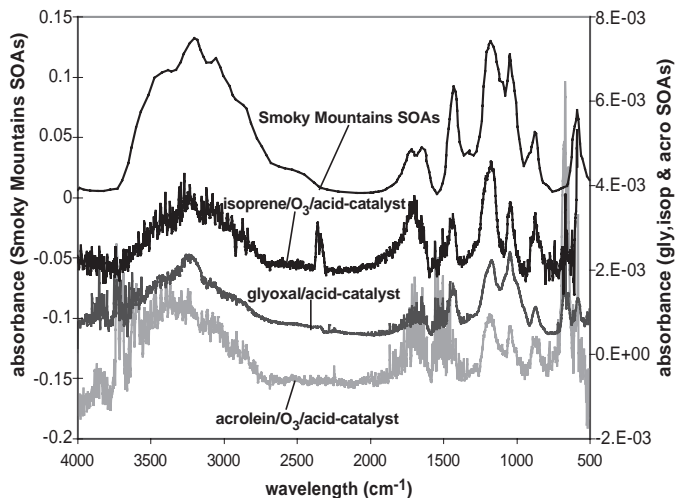


Fig. 4. FTIR spectra of organic aerosols impacted on an ungreased ZnSe FTIR disk for the glyoxal-(NH₄)₂SO₄-H₂SO₄ system and SOAs from the reaction of O₃ with isoprene and acrolein in the presence of an acid catalyst (H₂SO₄). The FTIR spectrum for SOAs from the Smoky Mountains was obtained from Blando *et al.* (37): FTIR spectrum of 0.5- to 1.0- μ m aerosols collected on 13 August 1995 at Look Rock, Smoky Mountains, Tennessee. Axis label E-03 indicates $\times 10^{-3}$.



spectra from size-resolved particle samples collected from the Southeastern Aerosol Visibility Study in the Smoky Mountains at Look Rock by Blando *et al.* (37) also show similar peaks at 589, 878, 1049, and 1182 cm⁻¹. This spectrum suggests that the organics comprising SOAs from the Smoky Mountains natural aerosol also have functional group transformations similar to those in our laboratory isoprene and acrolein aerosols. We believe that these transformations are due to acid-catalyzed heterogeneous reactions, which are therefore a major contributor to SOA formation in natural systems.

Our results strongly suggest that inorganic acids, such as H₂SO₄, catalyze carbonyl heterogeneous reactions and consequently lead to a large increase in SOA production. Thus, both inorganic and organic constituents need to be considered for an accurate explanation of SOA formation. For example, we believe that scenarios for high SOA formation and high concentrations of atmospheric inorganic acids may be coincident. Additionally, biogenic and anthropogenic emissions of carbonyl species associated with photooxidation cycles are considerable. Processing these carbonyl compounds via particle-phase heterogeneous reactions constitutes a previously unstudied, and to date unquantified, source of global aerosol material. The importance of quantifying global aerosol mass is key to understanding the climate forcing properties of aerosols. Thus, the role of heterogeneous reactions in SOA formation needs to be considered in climate change prediction models.

References and Notes

1. "Air quality criteria for particulate matter" [EPA/600/P-95/001cF, Environmental Protection Agency (EPA), Washington, DC, 1996].
2. R. L. Tanner, W. Parkhurst, *J. Air Waste Manage. Assoc.* **50**, 1299 (2000).
3. J. E. Hansen, M. Sato, *Proc. Natl. Acad. Sci. U.S.A.* **98**, 14778 (2001).
4. J. M. Adams, J. V. H. Constable, A. B. Guenther, P. Zimmerman, *Chemosphere-Global Change Sci.* **3**, 73 (2001).
5. A. P. Altshuller, *Atmos. Environ.* **17**, 2131 (1983).

6. H. E. Jeffries, in *Composition, Chemistry, and Climate of the Atmosphere*, H. B. Singh, Ed. (Van Nostrand Reinhold, New York, 1995), pp 308-348.
7. B. Noziere, I. Barnes, K. H. Becker, *J. Geophys. Res.* **104**, 23645 (1999).
8. R. M. Kamens, M. Jang, C. J. Chien, K. Leach, *Environ. Sci. Technol.* **33**, 1430 (1999).
9. J. Yu, H. E. Jeffries, K. G. Sexton, *Atmos. Environ.* **31**, 2261 (1997).
10. M. Jang, R. M. Kamens, *Environ. Sci. Technol.* **35**, 3626 (2001).
11. _____, *Environ. Sci. Technol.* **35**, 4758 (2001).
12. B. J. Finlayson-Pitts, J. N. Pitts, *Chemistry of the Upper and Lower Atmosphere: Theory, Experiments, and Applications* (Academic Press, New York, 2000), pp. 207-213.
13. H. J. Tobias, *Environ. Sci. Technol.* **35**, 2233 (2001).
14. M. S. Reddy, C. Venkataraman, *Atmos. Environ.* **36**, 677 (2002).
15. J. Curtius *et al.*, *J. Geophys. Res.* **106**, 31975 (2001).
16. J. R. Odum, T. P. W. Jungkamp, J. H. Seinfeld, *Science* **276**, 96 (1997).
17. T. Hoffmann *et al.*, *J. Atmos. Chem.* **26**, 189 (1997).
18. D. Barton, in *Comprehensive Organic Chemistry: The Synthesis and Reactions of Organic Compounds*, W. D. Ollis, Ed. (Pergamon Press, New York, 1979), pp. 960-1013.

19. H. J. Tobias, K. S. Docherty, D. E. Beving, P. J. Ziemann, *Environ. Sci. Technol.* **34**, 2116 (2000).
20. F. A. Carey, R. J. Sundberg, *Advanced Organic Chemistry: Part A Structure and Mechanisms* (Plenum Press, New York, ed. 4, 2000).
21. M. T. Nguyen, A. Jamka, R. Cazar, F. M. Tao, *J. Chem. Phys.* **106**, 8710 (1997).
22. H. W. Paerl, *Environ. Sci. Technol.* **36**, 323A (2002).
23. J. Kesselmeier, M. Staudt, *J. Atmos. Chem.* **33**, 23 (1999).
24. A. M. Winer *et al.*, *Atmos. Environ.* **26A**, 2647 (1992).
25. R. M. Kamens *et al.*, *Int. J. Chem. Kinet.* **14**, 955 (1982).
26. M. Jang, R. M. Kamens, K. Leach, M. R. Strommen, *Environ. Sci. Technol.* **31**, 2805 (1997).
27. J. F. Pankow, *Atmos. Environ.* **28**, 2275 (1994).
28. M. S. Reddy, C. Venkataraman, *Atmos. Environ.* **36**, 699 (2002).
29. M. Jang, S. Lee, R. M. Kamens, in preparation.
30. Gas-phase octanal was introduced with an air stream to the main body of the glass flow reactor (2.2-m length \times 2.5-cm inner diameter). The aerosol population sampled at ports spaced sequentially down the flow reactor was observed in the presence of an acid catalyst with a scanning mobility particle sizer. The %RH was varied by controlling the water-saturator. The experimental temperature was 295 to 296 K.
31. J. D. Blando *et al.*, *Environ. Sci. Technol.* **32**, 604 (1998).
32. Before the addition of hydrocarbons, seed aerosols were injected to the Teflon bags by nebulizing aqueous salt solution: 0.0067 M of (NH₄)₂SO₄ solution for nonacid seed and 0.005 M H₂SO₄ plus 0.0035 M of (NH₄)₂SO₄ for acid seed. Also note that the organic loss by the reaction on the wall surface will be higher as the molecular weight of aliphatic aldehydes increases.
33. The normalized aerosol yield for isoprene-O₃ was averaged from the data on 20 February 2001 and 24 February 2001. Two different sets of experiments on 24 February 2001 were used for the acrolein-O₃ systems. The initial O₃ concentration was 0.57 ppm. The experimental temperature was 295 to 296 K and %RH was 45 to 50%.
34. Supported by a grant from NSF (grant ATM 9708533) and a Science To Achieve Results grant from EPA (grant R-82817601-0) to the University of North Carolina at Chapel Hill.

Supporting Online Material

www.sciencemag.org/cgi/content/full/298/5594/814/DC1 Table S1

5 July 2002; accepted 20 September 2002

Robotic Observations of Dust Storm Enhancement of Carbon Biomass in the North Pacific

James K. B. Bishop,^{1*} Russ E. Davis,² Jeffrey T. Sherman²

Two autonomous robotic profiling floats deployed in the subarctic North Pacific on 10 April 2001 provided direct records of carbon biomass variability from surface to 1000 meters below surface at daily and diurnal time scales. Eight months of real-time data documented the marine biological response to natural events, including hydrographic changes, multiple storms, and the April 2001 dust event. High-frequency observations of upper ocean particulate organic carbon variability show a near doubling of biomass in the mixed layer over a 2-week period after the passage of a cloud of Gobi desert dust. The temporal evolution of particulate organic carbon enhancement and an increase in chlorophyll use efficiency after the dust storm suggest a biotic response to a natural iron fertilization by the dust.

Marine phytoplankton biomass is replaced, on average, once every 1 to 2 weeks (1-3). Carbon products of photosynthesis (4), i.e., particulate

organic carbon (POC), particulate inorganic carbon (PIC), and dissolved organic carbon (DOC), are exported below 100 m at a rate of

REPORTS

~ 10 Pg C year⁻¹. This process, commonly referred to as the ocean's "biological pump" (5, 6), is important to the regulation of atmospheric CO₂. The variability and linkages of the biological pump from surface to depth are poorly understood, because virtually all information on carbon dynamics within the upper kilometer of the ocean is derived from ship-dependent systems deployed for short periods of time (e.g., days to weeks).

Until recently, the use of optical instrumentation from drifting research platforms (7) and from deep ocean moorings (8–14) has been the only way to acquire long-term, uninterrupted high-frequency (hours or better), and depth-resolved time series measurements for detailed studies of biological and physical relations in the upper ocean on seasonal time scales. These observations provided clear documentation of a strong diurnal cycle in the abundance of particulate matter (7) and established the observational basis of an improved understanding of physical and biological process coupling in surface waters. Though ships and moorings are effective for deploying sophisticated instrumentation within regions or at individual sites, their costs limit their use for long-term monitoring on ocean basin or global scales.

The international program ARGO (15) has begun to seed the world's oceans with 3000 autonomous profiling floats to gather widespread temperature and salinity profiles and information on mid-depth circulation for investigation of the climate of the ocean. Such long-lived floats are designed to profile to the surface from kilometer depths once every 10 days over 5 years, and they have been already widely used to chart deep ocean circulation over basin scales (16). A faster derivative of the ARGO-style float (17) has been developed and equipped to measure POC (18, 19). Here we present carbon biomass variability of the North Pacific ocean obtained from first deployment of these floats, which we call Carbon Explorers (4).

Two Carbon Explorers were deployed from the U.S. Coast Guard ice breaker *Polar Star* in the subarctic north Pacific near Ocean Station PAPA (OSP; 145°W, 50°N) on 10 April 2001 (Fig. 1). Each was programmed to surface from depth at dawn, dusk, and midday on a repeating 2-day cycle (4) to capture net dawn-to-dusk POC production as well as data coincident with overpass of the sea-viewing wide field-of-view sensor (SeaWiFS) ocean color satellite (20). PAPA was chosen because its high-nutrient

low-chlorophyll (HNLC) waters have been well characterized for POC and beam attenuation coefficient (*c*) variability (19) as part of the Canadian Joint Global Ocean Flux Study (C-JGOFS) (21) and because PAPA is one of few sites in the world with a multi-decade-long time series of ocean observations relevant to the biological pump (22–25).

The two Carbon Explorers returned virtually unbroken data streams over 8 months of operation from April to December 2001 (4). Our longest-lived float completed nearly 400 profiles by 24 December 2001, at which time its batteries ran out. In this analysis, we focus on Carbon Explorer records from the first 50 days when the two profiling floats drifted within 40 km of each other and returned virtually identical records of POC variability (Fig. 2).

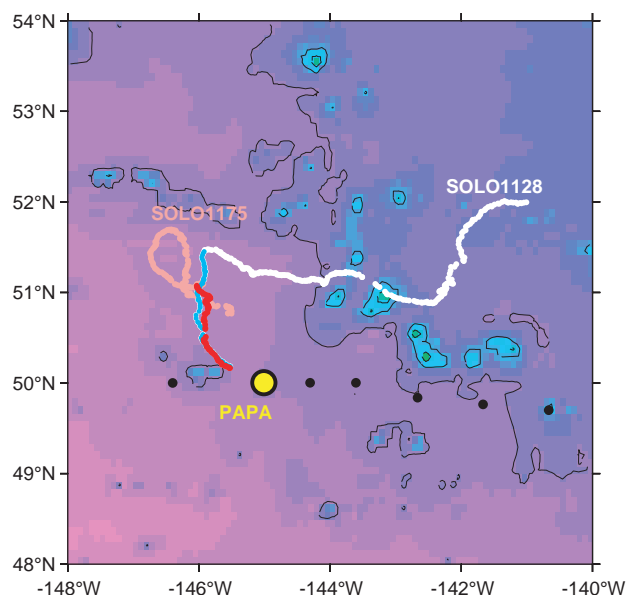
Throughout the first 50 days, the dawn mixed-layer depths ranged between <30 and 100 m (Fig. 2). There is a strong halocline at 100 m, suggesting isolation of the upper 100-m layer from beneath. POC is always highest in the surface mixed layer, and there is almost always a photosynthetic increase of POC in the mixed layer between dawn and dusk. The boundary between the particle-rich waters of the surface mixed layer and particle-poor waters below corresponds to the depth where the dawn profile potential density increases by 0.05 per mil (‰) relative to its surface value. This depth closely approximates the depth of greatest mixing during most days of the record and defines the "mixed layer" in discussions below.

A net photosynthetic production of POC in the mixed layer was recorded between dawn and dusk virtually every day throughout the

observing period (Fig. 2, bottom). The frequent return of the dawn POC to the previous day's morning values during many days of the record confirms the generally close balance between daytime primary productivity and day-long grazing in the waters at PAPA on a daily basis (24). There were times when net POC production appeared to exceed grazing. Daily POC increases frequently reached values of ~ 0.5 μM between days 110 and 118 (a 15% increase relative to dawn POC values); net gain over the following 30 days record averaged ~ 0.2 μM (typically $\sim 10\%$ of dawn POC levels), exceeding 0.3 μM only three times. Using the POC levels and dawn-dusk changes, we estimate a fast turnover time of POC in the mixed layer of 7 to 10 days. A natural consequence of the enhancement of rates of net POC production during days 110 to 118 is the observed build up of biomass in the mixed layer during those days.

The Carbon Explorers encountered two major storms in the first 50 days, when the mixed layer deepened rapidly to 100 m (Fig. 3). Average POC concentrations in the mixed layer were ~ 2.1 μM at the beginning of the study in April, typical of shipboard observations in 1996 and 1997 (19). Within 5 to 6 days after passage of the first storm (days 101 to 102), with thermal stratification, mixing depth shoaled to 50 m and POC began a steady increase over 10 days reaching peak levels of ~ 3.5 μM by day 118. During the second storm (days 119 to 121), POC concentrations dropped again to ~ 2.1 μM due to progressive entrainment of POC-poor subsurface waters as the mixed layer deepened twofold to 100 m. Another brief 1-day wind event

Fig. 1. Trajectories of SOLO Carbon Explorers over their lifetime (April to December 2001) superimposed over bathymetry (water depth near PAPA is greater than 4 km; black lines denote bathymetry contours at 1-km intervals). Cyan and red tracks denote trajectories for the first 50 days of deployment. White and pink tracks are trajectories of the floats from June to December 2001. The Carbon Explorers were deliberately placed to the northwest of OSP and were expected to drift eastward with the subarctic current. They drifted in the opposite direction from OSP for 3 weeks before turning northward and then finally turning east. Drift rates were 3 to 5 cm s⁻¹ during most of their 8-month deployment. They remained within 2 to 3 km of each other for 20 days; one float and then the other encountered a subsurface warm feature, and float separation increased to 40 km by 50 days. Black symbols are "line P" station locations (23) occupied during the C-JGOFS cruises.



¹Earth Sciences Division, Lawrence Berkeley National Laboratory, 1 Cyclotron Road, MS 90-1116, Berkeley, CA 94708, USA. ²Scripps Institution of Oceanography, La Jolla, CA 92093-0230, USA.

*To whom correspondence should be addressed. E-mail: jkbishop@lbl.gov

occurred on day 127. With restratification after the second period of stormy weather, there was a weak increase of POC to levels of $\sim 2.5 \mu\text{M}$ 10 days later (by day 136).

Photosynthetically active radiation (PAR) available for biological production in the water column varies with cloud cover, mixing depth, and particle concentration. Values fluctuating between 5 and 25 W m^{-2} were calculated (26) for the mixed layer (Fig. 3B). We identified two 10-day-long periods between storm events, centered on days 115 and 135, which had similar mixed layer stratification, high PAR, and constant salinity ($32.60 \pm 0.005 \text{ ‰}$; Fig. 3C). Yet these time periods had very different averaged mixed layer POC maxima ($\sim 3.5 \mu\text{M}$ and $\sim 2.5 \mu\text{M}$), suggesting that hydrographic and insolation changes alone cannot explain the high POC after the first storm (at day 118).

The growth of phytoplankton in HNLC waters near PAPA is believed to be limited

by the availability of iron for all or part of the time (22, 24, 27, 28). Fe demand by phytoplankton near PAPA is estimated to be $\sim 60 \mu\text{M Fe m}^{-2}$ on an annual basis (28). The total supply, $3 \mu\text{M Fe m}^{-2}$ from upwelling and $25 \mu\text{M Fe m}^{-2}$ from aeolian delivery (assuming an upper limit of 10% of the dust borne Fe is biologically available), falls short of the demand by at least two times.

Correlative analysis of different but not temporally coincident biogeochemical time series observations near PAPA (22) suggest that dust from the atmosphere could be the major iron supply. Lateral iron delivery from the continental margin, generally a result of river runoff and redox processes in shallow marine sediments, could also be a source of Fe to PAPA. This was ruled out in the correlative analysis because drifters deployed with a drogoue at 100 m moved from west to east consistent, with the general west-to-east flow of the subarctic current. Surface layer freshening is a

mid- to late-summer occurrence at PAPA (23) and was evident also in C-JGOFS observations collected in 1996 (19) and in the Carbon Explorer records in late July–early August 2001. Of the two Carbon Explorers, SOLO1128, which traveled further east, observed a lower and earlier salinity decrease than SOLO1175. Mixed layer POC reached as high as $5.5 \mu\text{M}$ in both Carbon Explorer records (not shown) with the peak coincident with the July–August arrival of a shallow 10- to 20-m-thick fresher layer with salinity $\sim 0.1\%$ lower than found at any other time of year. These observations suggest a likely summertime POC enhancement in response to seasonal continental runoff penetrating southwestward from the continental margin, with possible delivery of iron and micronutrients. However, with the mixed layer salinity remaining constant (within 0.005‰) between days 110 and 145, we rule out continental runoff as a contributor to the POC maximum near day 118.

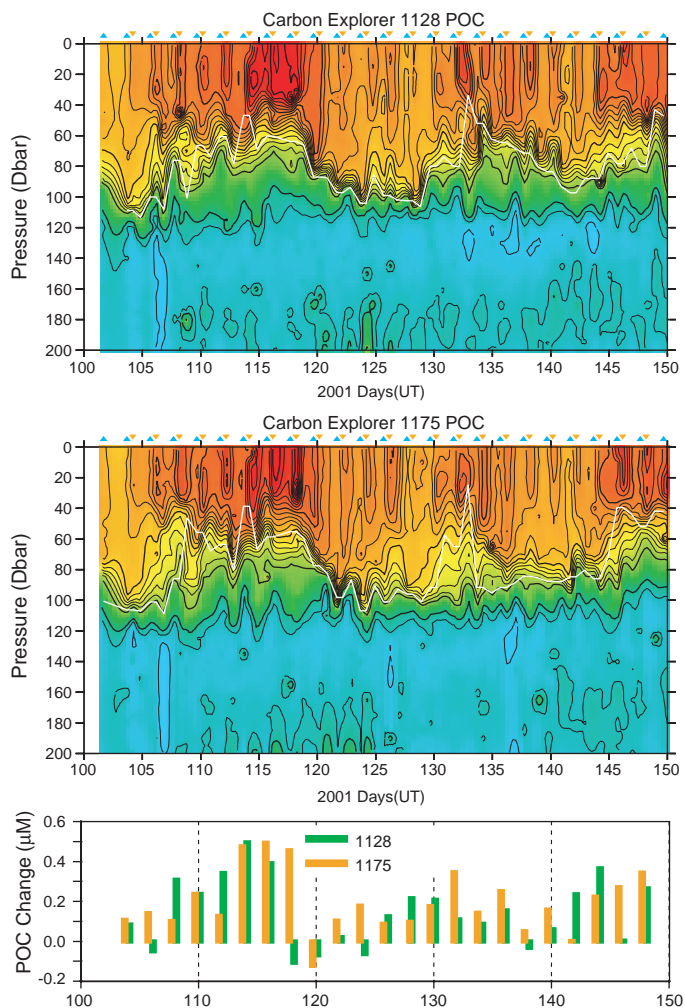
The first storm (day 101 to 102) encountered by the Carbon Explorers was a dust storm from Asia. Many details of this event are similar to the dust storm events of April 1998 (29). On 7 April 2001, the NASA TOMS satellite sensor recorded a large dust storm originating near the Gobi desert in southern Mongolia–northern China. The cloud of dust passed over Japan on 10 April (day 100), over PAPA on 12 and 13 April, and reached North America on 14 April 2001. The eastward decline of the TOMS aerosol index averaged for latitudes 50° to 52°N and longitudinal bands 165° to 155°W , 150° to 140°W , and 135° to 125°W suggests dust deposition to the oceans (Fig. 3A). Deposition was further indicated by the apparent lack of spatial dispersion seen in composite satellite images of the dust cloud as it passed these longitudes.

Therefore, the major dust input was on days 101 and 102. The POC loading in the mixed layer started to increase 5 days later, and peaked after 2 weeks (Fig. 3D). POC almost doubled between days 108 and 118. These higher values exceed, by a factor of two to four, the POC levels observed from ships in February of 1996 and 1997 and in May of 1996 (Fig. 3D) (19). The timing of the POC increase is similar to that found in purposeful addition of iron to cold southern ocean waters (30).

Chlorophyll retrievals by SeaWiFS (31) were sparse near PAPA during April and May 2001 due to nearly complete ($>92\%$) obscuration of the sea surface by clouds. The 11 usable images show a 25% chlorophyll enhancement between days 110 and 118 (Fig. 3D). Using Carbon Explorer and SeaWiFS observations, we estimate the POC/chlorophyll weight ratio for mixed layer particles to range between 60 and 80:1 (g C/g chlorophyll). The highest POC/chlorophyll ratio of 80 occurred during

Fig. 2. (Top and middle) Time series of POC variability from SOLO1128 and SOLO1175 during the first 50 days of deployment.

Cyan up-triangle and orange down-triangle at the top of each panel are plotted at the times of dawn and dusk profiles, respectively. On alternating days, a mid-day profile also contributes to the time series. Heavy black contours for cold to warm colors are drawn at 0.5, 1.0, 2.0, 3.0, and $4.0 \mu\text{M}$ POC levels. Light contours are at $0.2 \mu\text{M}$ spacing above $1.0 \mu\text{M}$ and at $0.1 \mu\text{M}$ spacing below $0.5 \mu\text{M}$. White curve is mixed-layer depth calculated from the dawn Carbon Explorer profile using a potential density increase of 0.05 relative to the surface. Mixing variability was consistent with surface winds retrieved twice per day using the JPL/QUIKSCAT instrument. Storms with winds persistently exceeding 25 knots occurred on days 101 to 102 and on days 119 to 122 and on day 127. Data contoured using GRI software. The “lock-step” nature of both records indicates that observed POC variability is a response to large scale forcing. (Bottom) Daily net growth or loss of POC calculated as dusk minus dawn POC averaged between the surface and depth of the dawn “mixed layer.” Enhanced net growth rates occurred on days 114 through 118 approximately 2 weeks after Gobi desert dust passed over PAPA.



the POC peak on days 116 to 118 and remained near 60 throughout the second storm and stratification period. The high ratio during the first stratification period is consistent with greater efficiency in nutrient utilization and biomass production as a result of reduced iron stress (28), analogous to observations of increased photosynthetic competency with the reduction of iron limitation (32).

The Carbon Explorer and SeaWiFS observations are, therefore, strongly supportive of the hypothesis of enhanced marine productivity, and enhanced carbon biomass in the euphotic zone, i.e., “fertilization,” in response to inputs of iron and other micronutrients from the Asian dust storm. Without Carbon Explorer observations before day 100, we cannot rule out definitively a preconditioning of the upper ocean that led to the enhanced bloom. However the POC/chlorophyll systematics strongly support an iron fertilization effect. It is evident that effects of the added Fe did not persist past 2 weeks, because there was only a weak growth of POC during the second 10-day-long stratification period.

Our observations of increasing POC levels following the likely natural fertilization of HNLC waters near PAPA indicates net pho-

tosynthesis increased faster than grazing and settling losses. The POC concentrations in deeper waters near 200 m show an increase near days 120 to 125 after the first surface POC maximum (Fig. 2). However, we cannot attribute this to dust-induced enhancement of organic carbon export from the euphotic zone to the deep sea, because our Carbon Explorers were not equipped to measure particle fluxes and we cannot distinguish between grazing and particle loss in the existing data.

All previous reports of dust and biological enhancement have relied on opportunistic observations made from ships at sea for very short periods of time (33–35). Strong dust events are highly episodic and affect the HNLC waters of the North Pacific near PAPA for a few days once every several years (22). It was only through analysis of hundreds of weekly surface chlorophyll observations made from weather ships at PAPA from 1961 through 1976, statistical seasonal probability analysis of wind trajectories and probable dust source regions, and a correlative comparison with 1984–89 records of carbon sedimentation at 3800 m that a very loose “link” was established between delivery of dust from the atmosphere and en-

hanced carbon export to the deep sea (22). The two Carbon Explorers provided, for the very first time, direct continuous observations of the upper ocean biological response to episodic events such as dust inputs and ocean storms. They have proven to be capable of sustained, high-frequency observations of carbon biomass variability in the ocean for the greater part of 1 year, thus greatly increasing the probability of directly observing biological responses to such episodic events.

This observational study with two autonomous floats supporting physical sensors and two bio-optical sensors demonstrates a potential for studying the carbon cycle on basin scales and multi-year time scales as well as some of the difficulties. Because the main carbon-cycle variability occurs in depth and time and is markedly decreased at depth, a time series of profiles is both descriptive and helpful in removing sensor drifts such as those caused by biofouling. Low cost, year-round operation and an ability for proliferation make autonomous floats particularly well suited to augmenting satellite observations by working under cloud cover, describing vertical structure, colocating multiple measurements, and making measurements more accurately than is possible with remote sensors. In contrast, autonomous instruments are not suitable platforms for many sophisticated measurements that require tending, use large amounts of energy, or are subject to biofouling (even at reduced levels achieved in this study). Ultimately, the challenge of carbon-cycle study will be observing with acuity the broad range of interacting variables over large space and time scales. Extensions of the Carbon Explorer concept should contribute.

References and Notes

1. C. B. Field, M. J. Behrenfeld, J. T. Randerson, P. G. Falkowski, *Science* **281**, 237 (1998).
2. P. G. Falkowski et al., *Science* **290**, 291 (2000).
3. P. G. Falkowski, R. Barber, V. Smetacek, *Science* **281**, 200 (1998).
4. Materials and methods are available as supporting material on Science Online.
5. T. Volk, M. I. Hoffert, in *The Carbon Cycle and Atmospheric CO₂: Natural Variations Archean to Present*, E. T. Sunquist, W. S. Broecker, Eds. (American Geophysical Union, Washington, DC, 1985), pp. 99–110.
6. A. R. Longhurst, W. G. Harrison, *Prog. Oceanogr.* **22**, 47 (1989).
7. D. A. Siegel, T. D. Dickey, L. Washburn, M. K. Hamilton, B. K. Mitchell, *Deep-Sea Res.* **36**, 211 (1989).
8. T. Dickey et al., *J. Geophys. Res.* **96**, 8643 (1991).
9. T. Dickey et al., *J. Geophys. Res.* **99**, 22541 (1994).
10. J. Marra et al., *J. Geophys. Res.* **97**, 7399 (1992).
11. M. Stramska, T. D. Dickey, A. Plueddemann, R. Weller, C. Langdon, J. Marra, *J. Geophys. Res.* **100**, 6621 (1995).
12. D. Foley et al., *Deep-Sea Res. II* **44**, 1801 (1998).
13. C. S. Kinkade et al., *Deep-Sea Res. II* **46**, 1813 (1999).
14. M.R. Abbott, J. G. Richman, R. M. Letelier, J. S. Bartlett, *Deep-Sea Res. II* **47**, 3285 (2000).
15. CLIVAR, *The Design and Implementation of Argo - A Global Array of Profiling Floats*, Report 21 (International CLIVAR Project Office, Southampton, UK, 1999), pp 1–35.

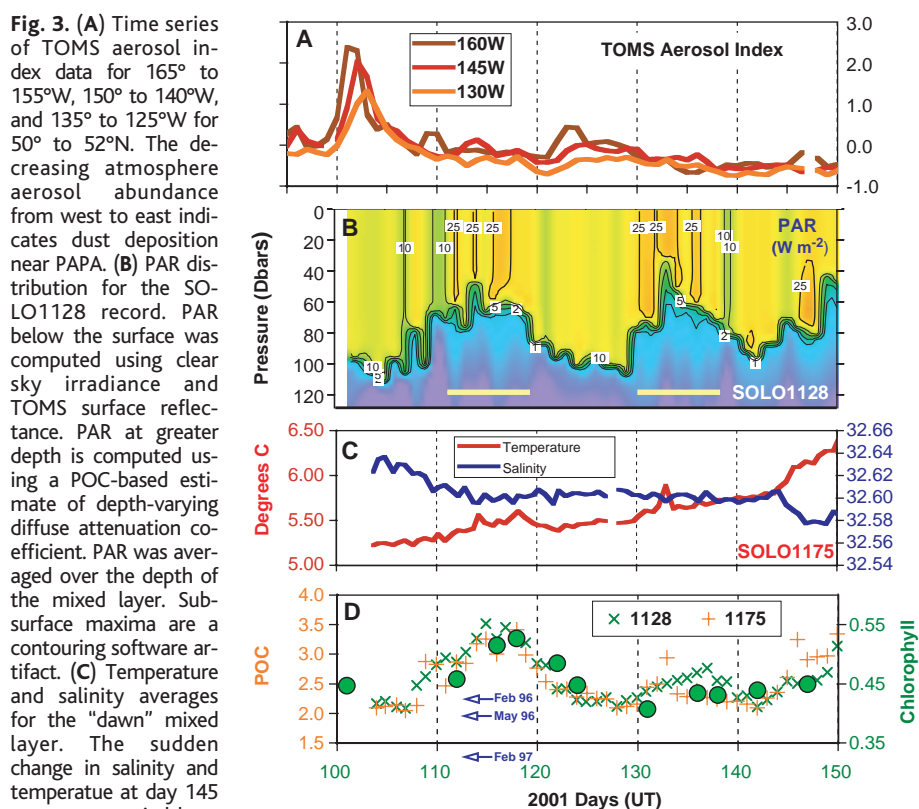


Fig. 3. (A) Time series of TOMS aerosol index data for 165° to 155°W, 150° to 140°W, and 135° to 125°W for 50° to 52°N. The decreasing atmosphere aerosol abundance from west to east indicates dust deposition near PAPA. (B) PAR distribution for the SOLO1128 record. PAR below the surface was computed using clear sky irradiance and TOMS surface reflectance. PAR at greater depth is computed using a POC-based estimate of depth-varying diffuse attenuation coefficient. PAR was averaged over the depth of the mixed layer. Sub-surface maxima are a contouring software artifact. (C) Temperature and salinity averages for the “dawn” mixed layer. The sudden change in salinity and temperature at day 145 was accompanied by a jump in POC. This is suggestive of lateral advection. Our analysis focuses on the first 45 days when the mixed layer appeared to be isolated as POC and temperature and salinity did not concurrently change. (D) Time series of mixed-layer “noon” POC variability for SOLO1128 and SOLO1175 and SeaWiFS chlorophyll retrievals for the first 50 days of record for a 200 km region near PAPA. POC is in units of μM. Chlorophyll is in units of mg m⁻³. Arrows denote POC levels from our C-JGOFs cruises from February 1996 and 1997 and from May 1996. The peaks in both POC and chlorophyll on days 116 to 118 (28 April 2001) are consistent with a biomass response to inputs of Asian dust and iron.

Human Occupations and Climate Change in the Puna de Atacama, Chile

Lautaro Núñez,¹ Martin Grosjean,^{2*} Isabel Cartajena³

Widespread evidence for human occupation of the Atacama Desert, 20° to 25°S in northern Chile, has been found from 13,000 calibrated ¹⁴C years before the present (cal yr B.P.) to 9500 cal yr B.P., and again after 4500 cal yr B.P. Initial human occupation coincided with a change from very dry environments to humid environments. More than 39 open early Archaic campsites at elevations above 3600 meters show that hunters lived around late glacial/early Holocene paleolakes on the Altiplano. Cessation of the use of the sites between 9500 and 4500 cal yr B.P. is associated with drying of the lakes. The mid-Holocene collapse of human occupation is also recorded in cave deposits. One cave contained Pleistocene fauna associated with human artifacts. Faunal diversity was highest during the humid early Holocene.

Initial Paleoindian occupation of southern South America is found in the temperate rain forest at 14,600 calibrated ¹⁴C years before the present (cal yr B.P.) (1, 2), but apparently 2000 years later at ~13,000 cal yr B.P. (3–5) in the arid Atacama Desert and on the coast of Peru. Does this reflect migration lags, prohibitive late Pleistocene environments, or an incom-

plete archaeological survey of the vast desert? Was Pleistocene fauna still present when the first people arrived? And did people respond to Holocene climate change?

Here we provide evidence that late glacial and Holocene human occupation in the Atacama Desert was associated with climate change. We surveyed the most arid part of the

16. R. E. Davis, *J. Geophys. Res.* **103**, 24619 (1998).
17. ———, J. T. Sherman, J. Dufour, *J. Atmos. Oceanic Tech.* **18**, 982 (2001).
18. J. K. B. Bishop, *Deep-Sea Res. I* **46**, 355 (1999).
19. ———, S. E. Calvert, M. Y.-S. Soon, *Deep-Sea Res. II* **46**, 2699 (1999).
20. J. E. O'Reilly *et al.*, in *SeaWiFS Postlaunch Calibration and Validation Analyses, Part 3*, S. B. Hooker, E. R. Firestone, Eds. (NASA Goddard Space Flight Center, Greenbelt, MD), pp. 1–49.
21. P. W. Boyd *et al.*, *Deep Sea Res. II* **46**, 2761 (1999).
22. P. W. Boyd *et al.*, *Global Biogeochem. Cycles* **12**, 429 (1998).
23. F. A. Whitney, H. J. Freeland, *Deep-Sea Res. II* **46**, 2351 (1999).
24. P. Boyd, P. J. Harrison, *Deep-Sea Res. II* **46**, 2405 (1999).
25. C. B. Miller, *Progr. Oceanogr.* **32**, 1 (1993).
26. PAR in the water column was calculated using clear sky irradiance (36), the daily surface reflectance data retrieved from TOMS data, and the diffuse attenuation coefficient estimated from the POC sensor (37–39). PAR was averaged over the mixed layer.
27. J. H. Martin, R. M. Gordon, S. Fitzwater, W. B. Broenkow *Deep-Sea Res.* **36**, 649 (1989).
28. I. Y. Fung *et al.*, *Global Biogeochem. Cycles* **14**, 281 (2000).
29. R. B. Husar *et al.*, *J. Geophys. Res.* **106**, 18317 (2001).
30. P. W. Boyd *et al.*, *Nature* **407**, 695 (2000).
31. SeaWiFS chlorophyll trends near PAPA were investigated by examination of retrieved chlorophyll values at 4-km spatial resolution over a region bounded by 49° to 52°N and 143° to 146°W from 1 April to 31 May 2001. Cloud cover exceeded 99% for 1 April through 10 April. Only 11 of 50 images available after 10 April had cloud fraction values below 85% and sufficiently clear views of the ocean for analysis. Histograms of chlorophyll data were examined and averages calculated after elimination of rare but very high (0.8 to 10 mg m⁻³) chlorophyll values which were found at cloud boundaries. To best match the SeaWiFS record, we averaged dawn and dusk mixed layer POC values obtained on odd days of our Carbon Explorer record and combined these with the "noon" data obtained on even days near the time of the SeaWiFS over pass (Fig. 3).
32. M. J. Behrenfeld, Z. S. Kolber, *Science* **283**, 840 (1999).
33. G. R. DiTullio, E. A. Laws, *Deep Sea Res.* **38**, 1305 (1991).
34. R. W. Young *et al.*, *Global Biogeochem. Cycles* **5**, 119 (1991).
35. J. M. Lenos *et al.*, *Limnol. Oceanogr.* **46**, 1261 (2001).
36. J. K. B. Bishop, W. B. Rossow, *J. Geophys. Res.* **96**, 16839 (1991).
37. C-JGFS POC/chlorophyll ratios in the mixed layer were approximately 70:1 (19, 38). As a rough approximation, we used chlorophyll estimated from POC data and the chlorophyll K relation of Smith and Baker (39).
38. D. Thibault, S. Roy, C. S. Wong, J. K. B. Bishop, *Deep-Sea Res. II* **46**, 2669 (1999).
39. R. C. Smith, K. S. Baker, *Limnol. Oceanogr.* **23**, 247 (1978).
40. We thank C. Moore and A. Derr (WETLabs) for developing the stabilized POC meter. The U.S. Coast Guard helicopter Todd Wood (LBNL) and the two Carbon Explorers from Dutch Harbor, the Aleutian Islands, to the icebreaker *Polar Star*, and assisted in the deployment of the floats in the North Pacific. P. Lam assisted with the analysis of SeaWiFS data. We gratefully acknowledge support from the National Oceanographic Partnership Program (NOPP) [N00014-99-F0450, N00014-99-1045, N00014-99-C-0449]; NOAA, Office of Global Programs [NA00AANRG0263]; LDRD of the Lawrence Berkeley National Laboratory; the Ocean Carbon Sequestration Research Program, Biological, and Environmental Research of the U.S. Department of Energy [KP1202030]; and NASA Ocean Biology/Biochemistry Program [NAG5-6450]. We thank the reviewers for their contributions.

Supporting Online Material

www.sciencemag.org/cgi/content/full/298/5594/817/

DC1

Materials and Methods

11 June 2002; accepted 17 September 2002

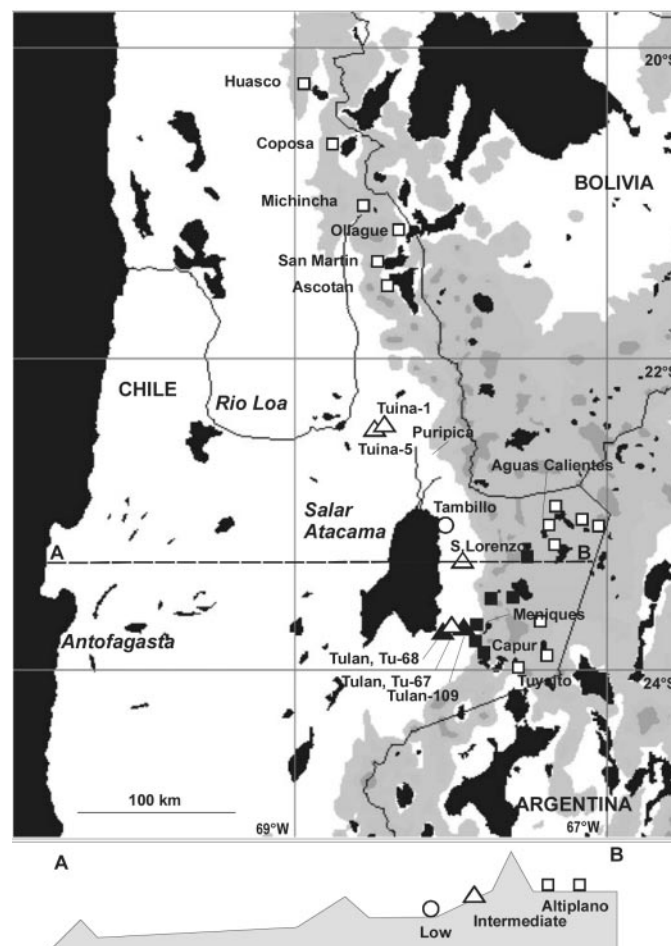


Fig. 1. Map showing the archaeological sites in high-elevation paleolake basins (squares), caves and shelters at an intermediate elevation between 3000 and 3600 m (triangles), and paleowetland sites at low elevation (2400 m) (circles). Lakes and salt flats in black shaded areas are above 4000 m. Open symbols are sites with triangulation points.